UNIVERSITY OF LEEDS

Article:
Connolly, DP, Dong, K, Alves Costa, P et al. (2 more authors) (2020) High speed railway ground dynamics: a multi-model analysis. International Journal of Rail Transportation. ISSN 2324-8378

https://doi.org/10.1080/23248378.2020.1712267

High speed railway ground dynamics: a multi-model analysis

David Patrick Connolly[a*], Kaitai Dong[b], Pedro Alves Costa[c], Paulo Soares[c], Peter Keith Woodward[a]

[a]Institute for High Speed Rail and System Integration, School of Civil Engineering, University of Leeds, UK
[b]Institute for Infrastructure and Environment, Heriot Watt University, UK
[c]Faculty of Engineering, University of Porto, Portugal

*Corresponding author

High speed railway ground dynamics: a multi-model analysis

High speed railway track and earthwork structures experience varied levels of displacement amplification depending upon train speed. Protecting against amplified track deflections is challenging due to the complexity of deep wave propagation within both the track and supporting soil structures. Therefore it is challenging to derive design guidelines that encompass the full range of influential variables. As a solution, this paper uses a novel multi-model framework where 4 complimentary modelling strategies are combined, and thus able to generate new insights into railway ground dynamics and 'critical velocity'. The four types of model are: 1) analytical, 2) hybrid analytical-numerical, 3) 2.5D numerical, 4) 3D numerical. They are used to explore subgrade layering, track type, train type, soil non-linearity, shakedown and ground improvement. The findings provide new insights into railway track-ground geodynamics and are useful when considering the design or upgrade of railroad lines.

Keywords: High Speed Rail; Railroad Critical Speed; Railway Track Deflection; Track Settlement; Railroad Geodynamics; Shakedown

1. Background

The typical operational speed of railway vehicles has increased in recent decades. This is problematic because increased dynamic track-ground amplification occurs when the train speed is greater than approximately 50% of the small-strain natural wave propagation velocity of the track-ground system.

To understand railway dynamics, first consider a moving, non-oscillatory load. If it moves at a speed equal to, or greater than the wave propagation velocity of any layer in the supporting track-ground, energy will propagate in the form of elastodynamic waves [1]. This minimum threshold speed is known as the 'critical velocity' [2–7]. Although additional factors can shift the speed at which maximum amplification occurs (e.g. multiple loads), the critical velocity definition never changes and must remain the minimum speed at which waves commence propagation.

Elevated levels of track dynamics are undesirable on railway lines because they pose a safety risk, result in accelerated track degradation [8], and can generate elevated ground-borne vibration in the free-field [9–13]. One example of where high dynamic track amplification was recorded is in Ledsgard, Sweden, where shortly after the opening of a new high speed line, abnormally large deflections were measured in the track [14–16]. This was expensive to remediate, requiring a combination of speed restrictions and soil remediation [17].

When designing lower speed lines it is important to consider the static stiffness of the track-ground system, however for high speed lines, the dynamic stiffness of the system must also be considered. Railway standards achieve this using empirical formulas, which typically consider the track behaviour as a combination of dynamic and static response [18]. However, these calculations are commonly a rudimentary function of the static response and speed, and thus unable to accurately account for the complex wave propagation due to differing track, ground and vehicle types. Therefore this approach is challenging to use for detailed design.

To investigate moving load dynamics, the problem has been modelled analytically, as a moving load over an elastodynamic medium, [19–21]. Alternatively, rather than explicitly simulate a moving load, the analytical dispersion characteristics of the track and ground can be analysed. This is useful from a scoping viewpoint because the speed at which the dispersion curves intersect is the critical speed of the track-ground structure [1,22].

Rather than pure analytical simulation, the problem has also been modelled semi-analytically (e.g. [23–25]), where the track is simulated analytically and the 3D soil is modelled using Green's functions in the wavenumber-frequency domain [23,26]. Using semi-analytical models, dynamic amplification factor (DAF) curves can be readily computed. These curves define the relationship between train speed and dynamic displacement amplification, thus requiring the model to be executed repeatedly for all discrete speeds.

Although semi-analytical models have relatively low computation requirements, they limit the complexity of the track that can be studied. Therefore an alternative is to use 2.5D models, which accurately capture 3D response, however assume the railway track is invariant in the direction of train passage [9,27–29]. When simulating ballasted tracks though, 2.5D models are unable to simulate individual sleepers. This can be overcome using periodic 3D models which discretise the problem into a series of discrete slices (e.g. sleeper bays - [30,31]).

Alternatively, fully 3D models [32] are useful when the track properties/geometry are complex, and solved in either the time or frequency domain. Solving in the frequency domain allows for the relatively straightforward implementation of absorbing boundaries (e.g. PML/BEM [33]). In contrast, time domain formulations [34–37] are attractive because they allow for the modelling of more complex non-linear material models and wheel-rail contact algorithms [38,39].

2. Numerical modelling

Table 1 shows the trade-off between computational efficiency and versatility, scaling from poor to excellent, for the most common modelling approaches used to study railway track dynamics. It is clear that it is challenging to use a single model to accurately analyse the full range of railway track dynamics. Therefore this paper links four alternative modelling methodologies to make new findings into critical velocity issues that are too time consuming to analyse using a single 3D model, and too complex for the use of solely simplified approaches. For all models, wheel-rail irregularities and vehicle multi-body dynamics are ignored due to their minimal influence on the low-frequency near-field response caused by high speed trains on straight track [40]. Note that although all four models have different levels of complexity, they all fully account for 3D wave propagation in the ground. This is important because 1D/2D approximations of wave propagation cannot typically provide accurate solutions for moving load problems. The methodologies used are discussed below.

Table 1. Comparison of common railway dynamics modelling strategies

Calculation approach	Computational efficiency		Computational versatility			
	Critical speed calculation	Dynamic amplification curve calculation	Deep soil wave propagation	Track geometry	Track-soil coupling	Soil non-linearity
Empirical	Poor	Lacking	Poor	Poor	Poor	Poor
Analytical dispersion	Excellent	Poor	Good	Lacking	Lacking	Poor
Semi-analytical	Good	Excellent	Good	Lacking	Good	Moderate
2.5D	Good	Good	Good	Good	Excellent	Good
3D (frequency domain)	Moderate	Moderate	Excellent	Excellent	Excellent	Good
3D (time domain)	Lacking	Lacking	Excellent	Excellent	Excellent	Excellent

Methodology 1 (Analytical): Analytical expressions for the dispersion relationships of both the track and ground are computed as outlined in [22]. This is advantageous because the critical velocity can be calculated in an automated fashion, in the absence of (computationally intensive) dynamic amplification curves. Figure 1 illustrates the dispersion curves in terms of both wavenumber and phase velocity, for a two-layered soil supporting a concrete slab track. The top layer is 5m thick and has a shear wave speed of 96m/s, while the bottom layer has a speed of 136m/s. In terms of phase velocity, it is straightforward to read that the critical velocity is 112m/s, however for the wavenumber representation, the following calculation is required: $v = f/k = 6.16/0.055 = 112m/s$. Therefore, for ease of use, phase velocity is used solely in this work.

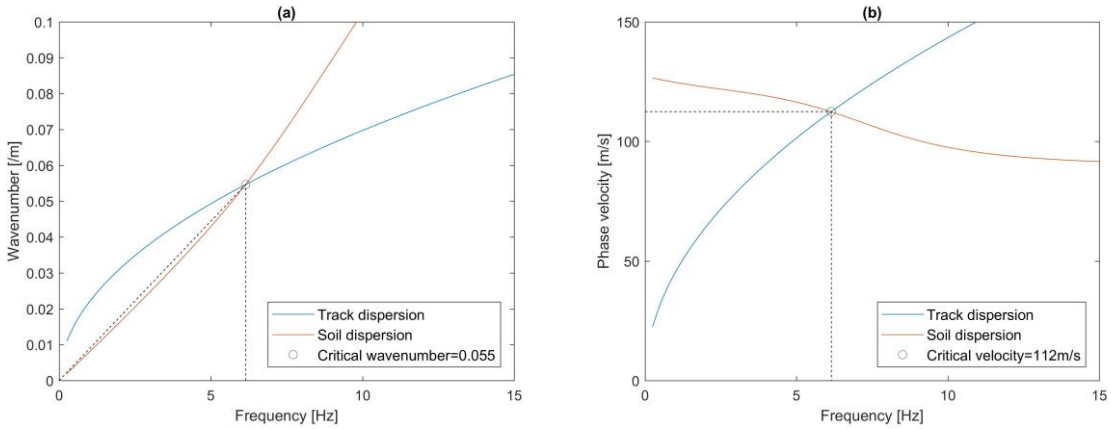

Figure 1. Dispersion relations: (a) Wavenumber, (b) Phase velocity

Methodology 2 (Combined analytical-numerical): The track is simulated using analytical expressions while the ground is modelled using the thin-layer element method (TLM). First the wavenumber-frequency domain displacement Greens function of the ground is computed,

using 8, 3-node quadratic thin-layer elements per wavelength. The Green's function is then used to compute an equivalent wavenumber-frequency dependent soil stiffness that is influenced by load speed, track type and width. This stiffness is then used within the track model to compute the coupled track-ground response as shown in Figure 2 - [41].

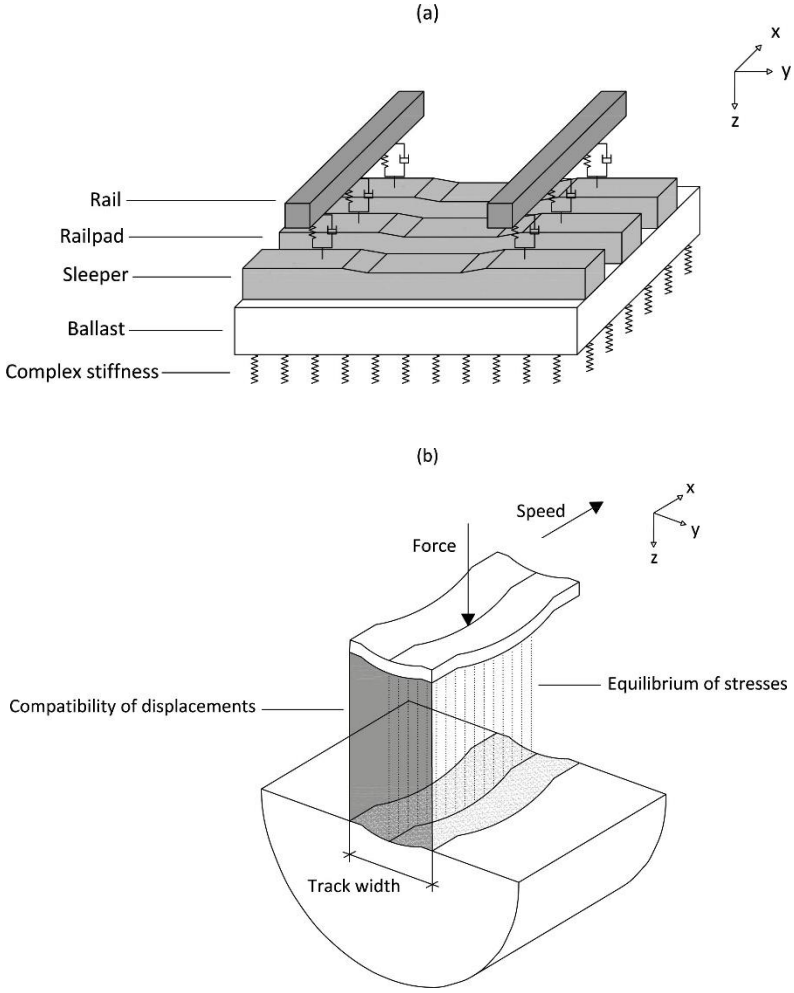

Figure 2. Semi-analytical: (a) track model, (b) track-ground interface

Methodology 3 (2.5D numerical): 8 node quadratic finite elements are used to define the 2D geometry of the entire track-ground structure [28,40]. Therefore the track and ground are fully coupled across their interface, without sub-modelling. Absorbing boundaries are used to prevent boundary reflections and the equations of motion are solved in the frequency domain (Figure 3). A transform is used to recover the 3D response.

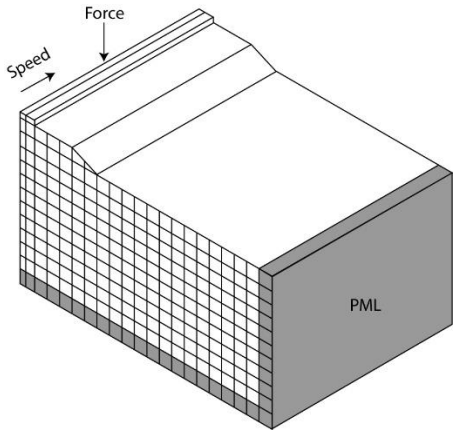

Figure 3. Simplified view of 2.5D track-ground mesh

Methodology 4 (3D numerical): Individual railway track components such as railpads and under-sleeper pads are modelled explicitly (Figure 4). 20 node quadratic brick elements are used for all track-ground components, thus ensuring the accurate modelling of stress and strain fields. The equations of motion are solved for moving loads in the time domain using ABAQUS [36,42].

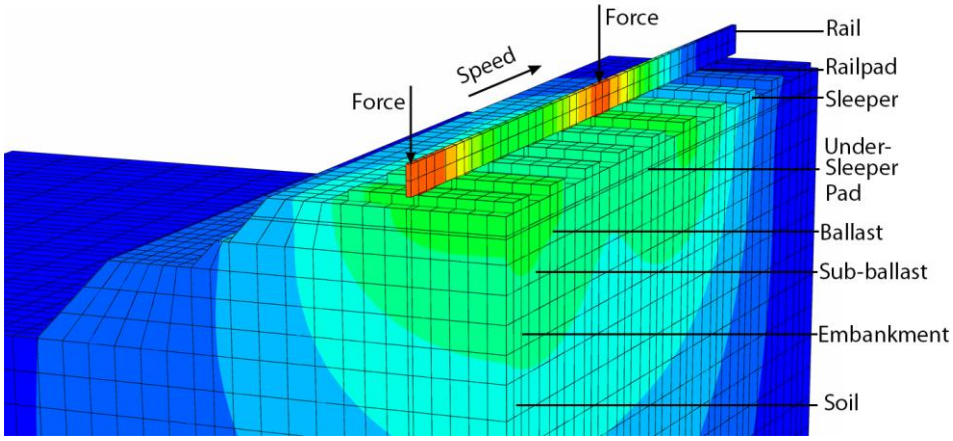

Figure 4. 3D ballasted track-ground model (Symmetrical quarter-track slice)

3. Numerical analysis

3.1 Modelling parameters

Static track-ground stiffness dominates track deflection response during slow train passage. However, when considering dynamic amplification due to high-speed train passage, deep wave propagation is induced and thus the dynamic stiffness characteristics of the supporting subgrade become increasingly important [43]. Therefore, although this analysis considers multiple track types, comparatively, a wider range of track stratums are explored. The track properties used throughout, unless otherwise stated, are shown in Table 2. Regarding soil properties, rather than focus on a single generic stratum throughout, the Young's modulus is changed in each individual section for the purpose of informing the discussion. However, the

Poisson's ratio and density are kept constant at 2000 kg/m^3 and 0.35 respectively. Regarding analysis layout, the most straightforward problems (e.g. soil layering) are presented first, followed by problems of increasing complexity.

Table 2. Track material properties

Component	Ballasted track	Slab track	Description
Rail	1.29x10^7	1.29x10^7	Bending stiffness (Nm^2)
	120	120	Mass (kg/m)
Railpad	5x10^8	5x10^8	Stiffness (N/m)
	2.5x10^5	2.5x10^5	Damping (Ns/m)
Sleeper	490	-	Mass of sleeper (kg/m)
Ballast/slab	0.35	0.35	Height of ballast/slab (m)
	130	30,000	Young's modulus (MPa)
	1.25	1.25	Half-track width (m)
	1700	2500	Density (kg/m^3)

3.2 Homogenous half-space soils

A homogenous half-space is a soil stratum with uniform material properties that extends to infinite depth. Its uniform stiffness and mass mean that the P-SV phase velocity is independent of excitation frequency, and as such, the critical velocity is equal to the Rayleigh wave velocity. Although it is rare that the behaviour of an in-situ soil can be accurately approximated this way, due to simplicity it is the most commonly assumed type of soil stratum in track design practise.

Figure 5 shows the ground contours of a homogenous half-space (45MPa stiffness) that supports a moving train wheel load on a ballasted track (properties in Table 2). Two different speeds are shown: one at 50% of the Rayleigh wave velocity and one at 100% of the Rayleigh velocity. It is clear that the faster load produces significantly larger deflections (maximum rail deflection is 2.5mm and 3.9mm for the slow and fast speeds respectively). Also, there is a distinct discrepancy between response contour shape – the lower speed produces a uniform response, while the faster speed produces a conical-type shape. At speeds greater than the Rayleigh wave speed, this wave-front angle is defined by: $arcsin(V_{Rayleigh}/V_{train})$.

Similarly, Figure 6 shows the corresponding stress fields generated at 1m below the surface. Principal stress rotation is evident at both speeds, and the low speed stress fields are consistent in shape with the literature [44]. However, at the faster speed, the stress fields develop asymmetry and are larger in magnitude. These changes are found for all stress components, but particularly in the horizontal directions, and is one reason why it is challenging to develop empirical approximations of soil non-linearity (and thus soil stiffness reduction) at high speed.

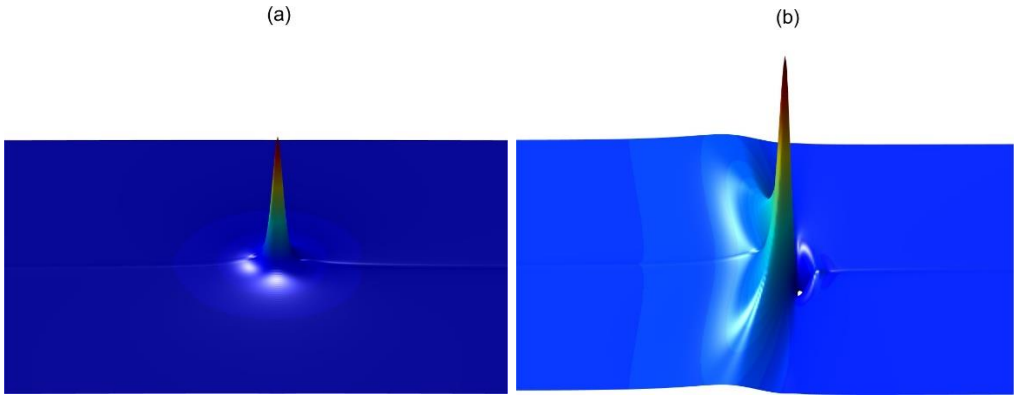

Figure 5. Homogenous ground contours for a load moving from left to right: (a) 50% of critical speed, (b) critical speed

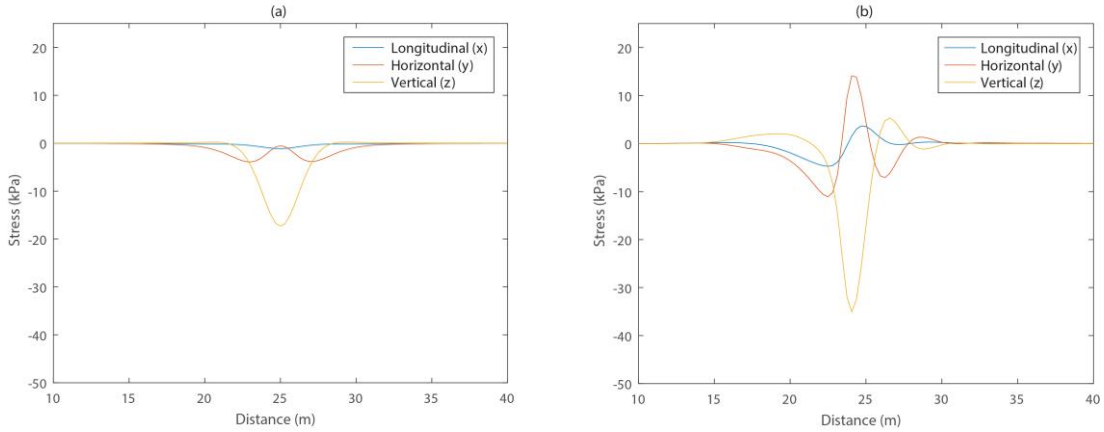

Figure 6. Soil stresses: (a) 50% of critical speed, (b) critical speed

3.3 Homogenous soils above bedrock

Soil stratums typically increase in stiffness with depth due to historical earth pressures. If a layer is found near the surface with significantly higher stiffness (e.g. rock) than the soil it supports, it will reflect wave energy while also preventing lower frequencies from propagating. Figure 7a shows the dispersion and displacement characteristics of a slab track resting on homogenous saturated and unsaturated 40MPa soils, supported at depths of both 5m and 15m by stiff bedrock. The presence of the bedrock prevents low frequency waves from propagating, as shown by the dashed lines. This is because low frequency waves have a longer wavelength than the bedrock depth, and as such, the bedrock prevents their propagation. If V_s is shear wave speed and d is bedrock depth, the 'cut-on' frequency is computed as: $f_{cut-on} = \frac{V_s}{4d}$.

Figure 7a shows significant dispersion (i.e. high phase velocity versus frequency gradient) in the 5-10Hz range for the 5m deep bedrock case and in the range 1-3Hz for the 15m deep bedrock case. This results in highly contrasting critical velocities for the 2 different bedrock depths. Therefore it can be concluded that if the critical velocity occurs in a highly dispersive frequency range, small changes to the track stiffness can have marked

changes on the critical velocity. Conversely, at higher frequencies (e.g. >5Hz for the 15m soil case and >12Hz for the 5m case), the relationship between phase velocity and frequency is constant, indicating that if the critical velocity lies within this range, altering the track stiffness properties will not change the critical speed.

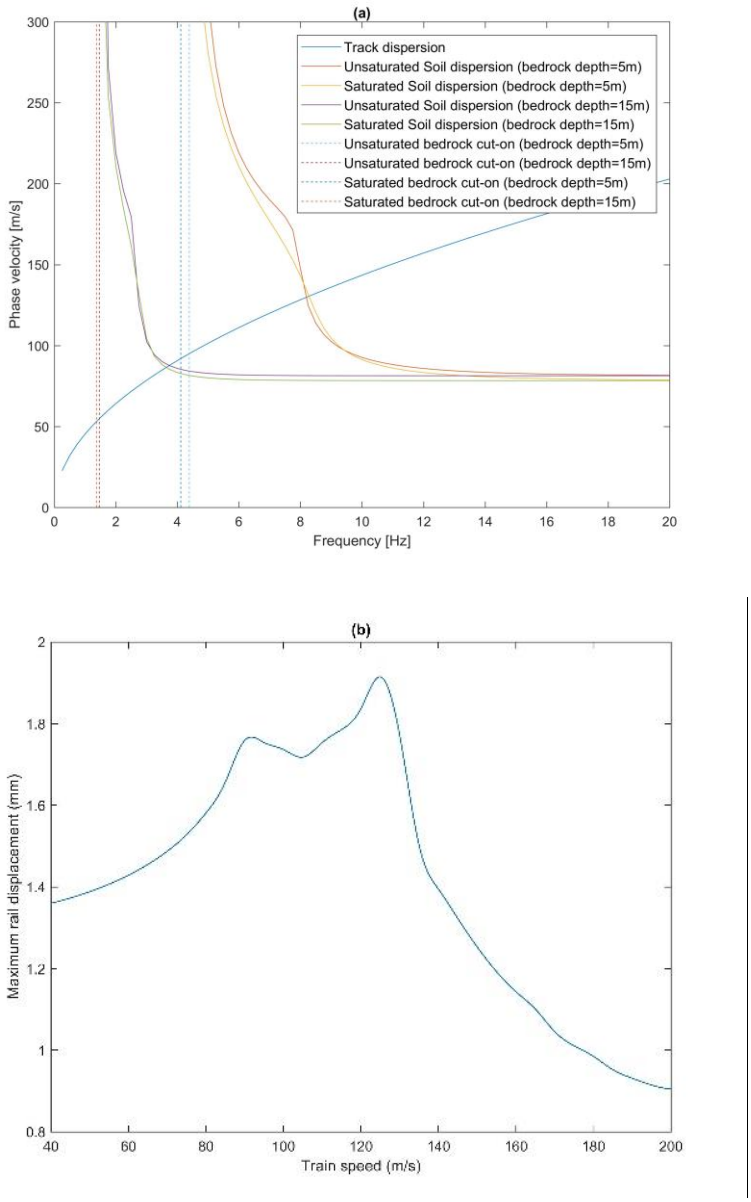

Figure 7. Critical velocity: (a) the effect of bedrock depth of dispersion, (b) Maximum vertical rail displacement curve in the presence of a low velocity sandwich layer

3.4 Layered soils

In contrast to the homogenous and bedrock cases presented previously, layered soils are defined in this section as infinitely deep soils (i.e. no bedrock support) with a soil stiffness profile that varies with depth. First consider a slab track resting on six different two layered soils. The lower soil layer has a stiffness of 150MPa, while the top layer is varied between 30, 75 and 100MPa. For each stiffness case the top layer is either 'thick' (12m) or 'thin' (2m). Figure 8 shows the ground contour plots for the slab track on the thick 30MPa layer

overlying the stiffer layer. The speeds are 50% and 100% of the critical velocity, and in a similar manner to the homogenous case, the faster moving load causes higher displacements (maximum rail deflection is 3.9mm and 4.9mm for the slow and fast speeds respectively). However, also noticeable is the presence of trailing oscillations behind the faster load. These are caused by the dispersive characteristics of the layered soil. The homogenous case will never exhibit these regardless of moving load speed.

To analyse the effect of dispersion in more detail, Figure 9a shows the track-ground dispersion for each case. It is seen that when the top layer is thick, the critical velocity is similar to the P-SV wave velocity in the top layer, and quite different to the wave velocity in the lower layer. This occurs because the intersection is located in a range where phase velocity and frequency are have a constant relationship. Therefore changes to the track have limited effect on critical velocity. This is generally true when the top layer thickness is deep, however can change if there is a very strong contrast between top and bottom soil stiffness.

In contrast is the case of the shallow upper layer. For this case, the critical velocity is located between the P-SV wave speed of the upper and lower layers. Typically, as the thickness of the top layer reduces, the critical speed will diverge towards the wave speed in the lower soil layer. Again, however, this is dependent upon the shear wave profile with depth [45].

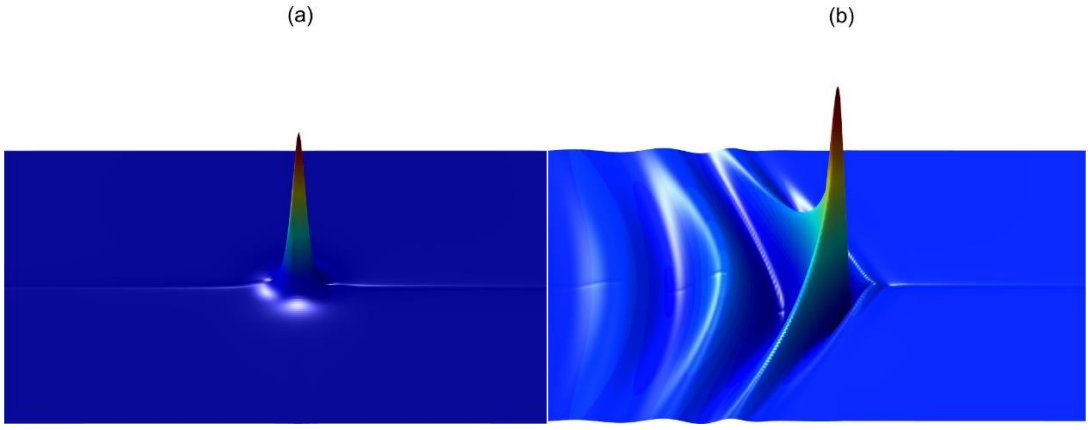

Figure 8. Layered ground contours for a load moving from left to right: (a) 50% of critical speed, (b) critical speed

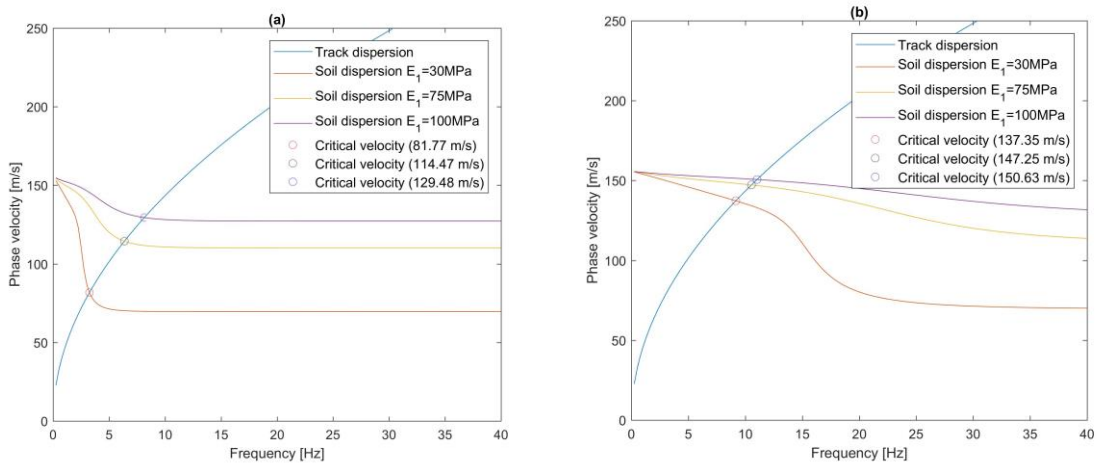

Figure 9. Layered soil dispersion: (a) thick upper layer -12m, (b) thin upper layer-2m

3.5 Sandwiched low stiffness soil layers

The earth's upper crust typically increases in stiffness with depth due to historical earth pressures. However, interim low-stiffness layers can occur either naturally [16] or due to localised soil improvement [41]. In this case, unlike the previously considered scenarios, the soil phase velocity will increase with frequency rather than decrease. This presents challenges for track and earthwork design because:

1. Inversely dispersive P-SV modes are generated, possibly causing additional DAF peaks that hold more energy than the critical velocity peak
2. The low stiffness zone is located below the top surface layer, thus making remediation costly
3. Dispersion curve analysis is more challenging and the inversion algorithms associated with many typical ground surveys are not well-suited for detecting higher modes. Therefore, in absence of experienced human interpretation, their presence may be overlooked or misinterpreted

As an example of multiple DAF peak generation, Figure 7(b) shows 6m of moderately stiff soil (100MPa) overlying a softer and infinitely deep soil (50MPa). It is seen that two peaks occur, at similar speeds to the shear wave velocities of the two soil layers. The first peak, by definition, is the critical velocity because it is the speed at which elastodynamic wave energy commences propagation (in the lower layer). However a train running at the speed of the second peak will generate highest track amplification.

3.6 Saturated soils

Efficient railway line operation relies on free-draining track and subgrade. However, this is not always the case and if the subgrade voids fill with water, its Poisson's ratio will increase to 0.5. This results in a large increase in compressional wave speed (to a speed more comparable with water), and a minimal increase in shear wave speed because water has no shear strength. Therefore, because the Rayleigh wave velocity is a function of the shear wave

speed, it also does not change significantly. The normalised relationships between wave speeds due to changes in Poisson's ratio, when the shear wave speed is held constant, are shown in Figure 10.

For the majority of cases, saturation will lower the critical velocity. However, if a soil is layered, its dispersion characteristics determine whether high saturation will increase or decrease the critical velocity. For example, Figure 10b shows a soft, 2m thick soil layer with Young's modulus 25MPa, over a stiff, infinitely deep soil layer with a Young's modulus of 100MPa. In this case the critical velocity lies in a zone where there is significant dispersion and thus the critical velocity is slightly higher for the saturated soil compared to the unsaturated soil. This is due to the high contrast in stiffness between the upper and lower layers. In practise however, soil layers are likely to have less contrasting stiffness values, and thus the saturated soil would more commonly yield a lower critical velocity. Also, note that despite any possible benefits of soil saturation on critical velocity, the presence of water will likely cause other track problems, outside the scope of this paper.

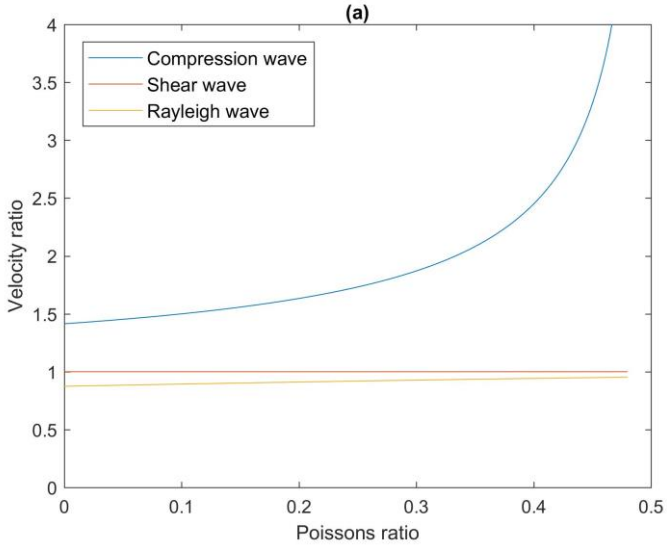

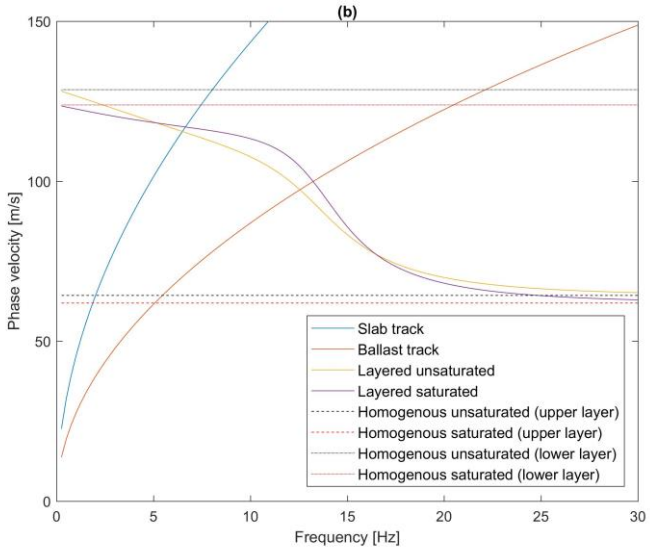

Figure 10. The effect of soil saturation, Left: wave speeds in a homogenous half-space, Right: dispersion analysis

3.7 Track type

Waves propagating along a slab track do so at a higher velocity for a given frequency, compared to a ballasted track. This is due to the slab's higher bending stiffness and can be seen in Figure 10b which compares dispersion curves for the ballasted and concrete slab track. The critical velocity therefore occurs at a lower frequency for slab tracks, meaning deeper soil layers are more likely to affect slab critical velocity than ballast. In reality, because deeper soil layers increase in stiffness with depth, this is partly why slab tracks often have a higher critical velocity than ballasted. This is dependent on the shape of the soil dispersion curve though, and a thick upper soil layer will result in similar critical speeds for both ballast and slab tracks. As an extreme example, consider an infinitely deep homogenous soil, which therefore has a straight and horizontal ground P-SV dispersion curve. This means the track-ground dispersion intersection must always occur at a constant value, and thus the critical velocity is not altered by changes to the track structure. This is true for the range of typical track thickness values found in practise, however if the track thickness is large, the wave propagation within the track can potentially shift the critical speed for homogenous soil cases (and thus should not be computed solely using analytical dispersion curves).

3.8 Train axle configuration

In practical situations, rail vehicles are connected via multiple wheelsets which may interact depending upon their spacing and the supporting track-ground properties. Multiple wheels cause a combination of constructive and destructive interference which can yield dynamic amplification curves with significantly different magnitude and shape to those for a single wheel case. In particular, multiple dynamic amplification peaks are easily generated. These are not additional critical velocities, because the critical speed is independent of the moving load, as defined earlier.

When the soil stiffness is soft, track and ground displacements return to their equilibrium position more slowly than when the soil is stiff. Similarly, when approaching critical velocity, the deflection bowls below wheels elongate, and wheels that are closely spaced experience superposition – this has been observed both numerically and in field data [16,46]. Constructive interference is shown in Figure 11 for a 2-axle load moving at critical velocity on both a homogenous and bedrock supported soil.

As a practical example, consider Table 3, which divides common high speed train axle configurations into 6 categories. Axle spacing values are approximated from [47] and all vehicle axle loads are 18t. These axle loads are untrue for the real-life vehicles considered meaning true amplification for each will differ from Figure 12a however it provides an interesting way to isolate wheel spacing effects. 'Axle spacing 1' corresponds to the minimum spacing, while 'axle spacing 2' corresponds to the next possible minimum spacing. The response of each vehicle is computed, considering a ballasted track on a soft two layered soil consisting of a 3m thick layer with stiffness 50MPa, overlying an infinitely deep soil with stiffness 100MPa. Figure 12a shows how track response changes with speed for the different

axle configurations (for 4 wheel vehicles) compared to a single axle load. It is clear that the different vehicle configurations influence displacement response, particularly as speed increases. Also, in general, when considering multiple axles, the maximum displacements are higher, with the zones of elevated displacement covering a wider range of speeds. Multiple, localised peaks appear that are not present for the single load case. The first peak for vehicle 'f' corresponds to the critical velocity while the first peak for the other vehicles is higher. This is due to the complex interaction between individual axles and is interesting considering axle spacings 1 and 2 are high compared to several alternative other vehicles.

Although it is rare for trains to operate above critical velocity, in such a case, it should also be noted that resonance can occur due to coincidence between axle spacing wavelength and the free-vibration wavelength of the track-ground structure [46]. This constructive interference is evident in Figure 11b where the free-vibration wavelength and vehicle axle spacing are both equal. Significant constructive interference is observed. This only occurs in layered soils at speeds very close, or above the critical velocity because otherwise the soil does not have a natural frequency and free-vibration of the track does not occur (e.g. Figure 11a).

To illustrate the effect of resonance on layered soils, Figure 12b compares ballasted track maximum vertical rail displacement due to either critical velocity or resonance, for a 10-axle vehicle on a 50MPa soil with bedrock at 2m depth. The axle spacing is computed dynamically depending upon train speed, to ensure it is equal to the free-vibration frequency of the track-ground system. Comparing the low train speed deflection values against the higher speeds where critical velocity and resonance occur, it is seen that the amplification of rail displacement reaches a maximum ≈400%. In contrast, when only considering critical velocity, maximum rail amplification is <100%.

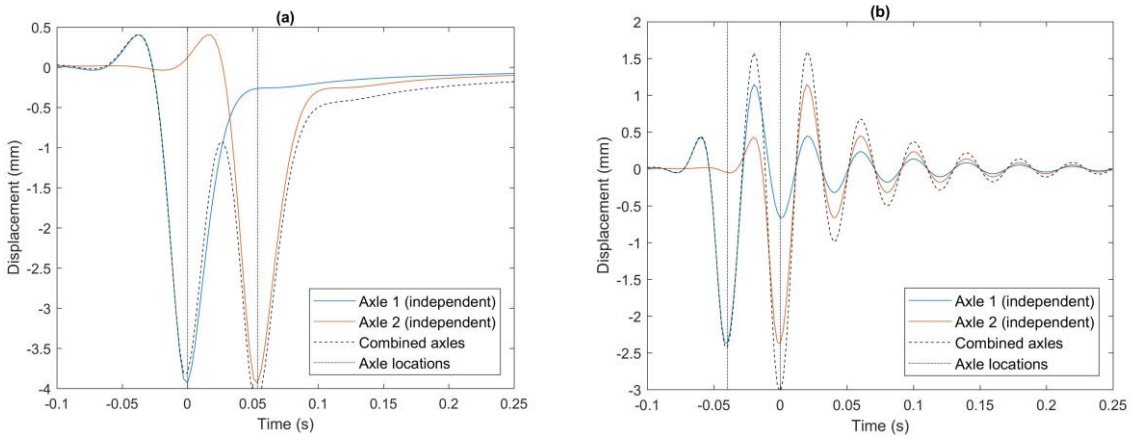

Figure 11. Displacement superposition at critical velocity: (a) Homogenous soil, (b) Layered soil

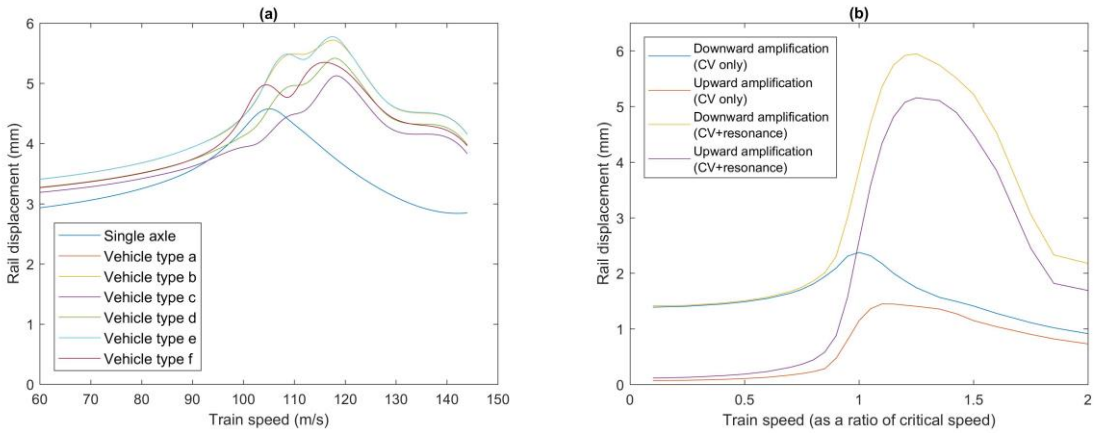

Figure 12. (a) DAF for different vehicles, (b) effect of train speed and resonance on rail displacement

Table 3. Vehicle axle configurations

Category	Indicative vehicle	Assumed axle load (tonnes)	Axle spacing 1 (m)	Axle spacing 2 (m)
a	TGV/Eurostar/Thalys/AVE S-100	18	3	3.14
b	ICE/AVE 103	18	2.5	3.7
c	Alfa Pendular	18	3.1	3.45
d	X2000	18	2.9	3.63
e	Javelin 395	18	2.6	2.91
f	Talgo 250	18	2.8	6.87

3.9 Track-soil non-linearity

As train speed increases, elastodynamic wave energy propagates to greater depths within the soil. This energy causes elevated strain levels, which may lie in the 'large-strain' range, resulting in non-linear soil-stiffness degradation during train passage. This reduced soil stiffness causes increased track deflections [48].

As an example, Figure 13 shows a track slice of the stiffness degradation contours computed at Ledsgard, Sweden, during the passage of a X2000 train at 204 km/h [28]. Assumed soil plasticity and confining stresses are detailed in [40]. It is clear that significant soil non-linearity is present and affects soil to large depths (<≈7.5m) and to large track offsets (<≈23m).

Similarly, as another example, Figure 14a shows linear and non-linear dynamic amplification curves for a moving 18 axle load on a homogeneous soil of stiffness 45MPa. The track properties are the same as shown in Table 2 and the degradation curves are the same as previously. The dynamic amplification has increased while the critical speed has been reduced to 85% of the linear case. It should be noted though that the response is highly sensitive to the soil properties. This is important because high speed rail lines often try to

limit train speed to 70% of the critical velocity, but due to non-linearity, in some cases, running at 70% of the linear calculation could yield the highest possible track deflections (or at least create a condition where deflections are extremely sensitive to small increases in speed). In addition, Figure 14b shows the corresponding relationship between strain and depth for speeds of 10m/s and 80m/s, computed using the linear equivalent approach. It is seen that at high speed the strains are significantly larger (387% at 1m depth) and propagate to greater depth, however the depth of peak strain remains similar.

Figure 15 also shows the p-q stress paths at a depth of 1m below the track centre-line for a low speed (10 m/s) and critical velocity (80 m/s). At a speed of 10m/s, there is no sign of dynamic amplification. However, when the speed reaches 80 m/s, the stress state becomes highly turbulent and the magnitudes increase significantly. It is important to note that non-linear effects are very sensitive to changes in vehicle axle configuration/load - much more so than the linear cases shown previously. When soil non-linearity is simulated, the linear superposition of axle response is invalid, meaning the non-linear amplification curve shown in Figure 14 is only valid for a single axle arrangement. This means that certain axle configurations can act to magnify dynamic amplification, and reduce the speed which induces maximum track deflection.

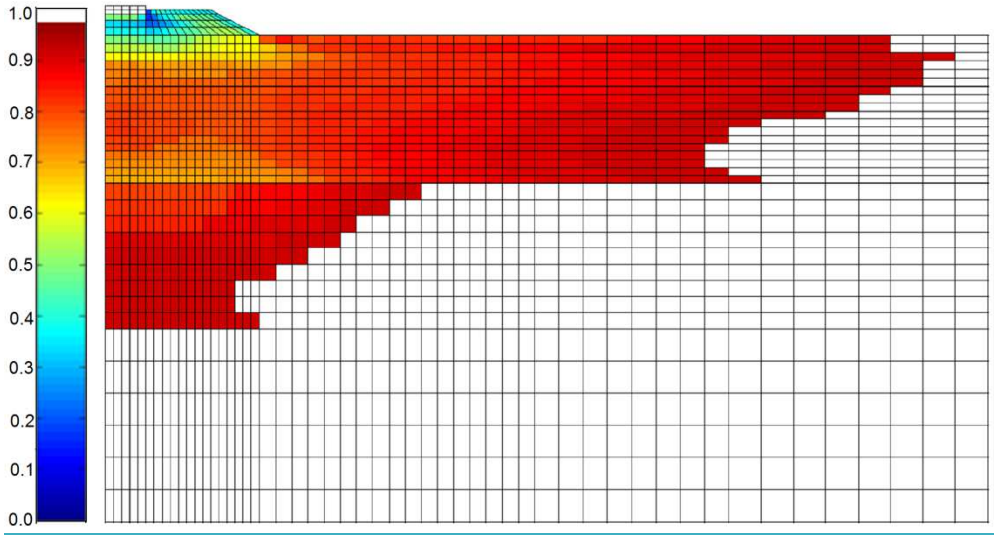

Figure 13. Track-ground non-linearity (Track slice). Blue colour indicates high stiffness degradation and white indicates low stiffness degradation [28]

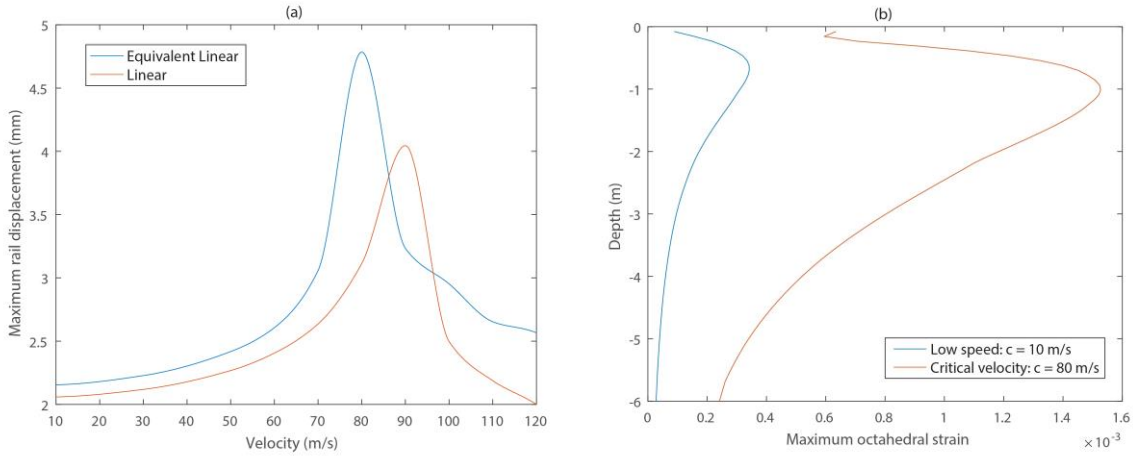

Figure 14. Effect on non-linearity: (a) Rail displacement vs speed, (b) Strain vs depth

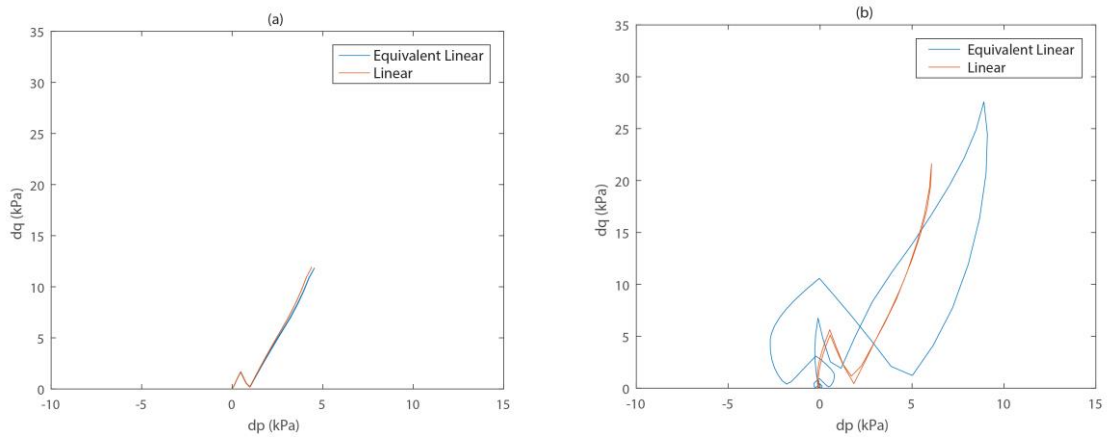

Figure 15. p-q stress paths: a) below critical speed (10m/s), b) critical speed (80m/s)

3.10 Track shakedown

During train passage, the track may experience a combination of elastic (recoverable) and plastic (non-recoverable) deformations [49]. Its response to repeated passages can be classified as shown in Figure 16a [45,50–52]:

Elastic: Train loading is low meaning the elastic yield limit is not exceeded. Track behaviour is fully elastic with no residual strain accumulation, meaning permanent settlement does not occur.

Elastic shakedown: Train loading is high, thus exceeding the yield limit for a limited number of initial train passages. This causes the track to settle, however soon after, the response returns to elastic again. Further passages do not result in additional permanent settlement accumulation unless the load is increased. This happens because the total stress field (i.e. residual stresses accumulated during the initial load cycles, combined with both the at-rest stress field and incremental stresses due to train loading) does not violate the yielding criteria.

Cyclic plasticity and ratcheting: Train loading is so high that the stress field induced by the train passage is greater than the elastic limit, thus inducing permanent strains during each train passage. This means that track permanent deformation does not stabilize, resulting in ever increasing track permanent settlement and ultimately failure.

The elastic shakedown limit is a term used to define the minimum load that will result in track failure. It is affected by the material properties of the track and subgrade, but also by the train loading characteristics (e.g. speed and geometry). In particular, if high levels of track dynamics are induced during train passage, then stresses are amplified (Figure 15), causing a reduction in the shakedown limit [53]. This is shown in Figure 16b, where the relationship between train speed and shakedown limit is plotted, for a homogenous ground with 71MPa Young's modulus and varying friction angles, φ=20^o, 25^o, 35^o. It is seen that the shakedown limit is highly sensitive to speed, with a minimum value found at the critical velocity (116m/s). Therefore track failure is most likely at this speed. For a 180kN axle load, if the moving load speed is low the factor of safety is 4.4, however at critical speed it is only 1.6. Note however that the y-axis indicates the shakedown limit for a single moving load, and will likely be reduced further when considering full train geometries.

This approach provides a practical tool to aid track design. As an example, current railway track design aims to limit train speeds to 65-70% of the critical velocity, independent of vehicle axle load and geometry. Alternatively, shakedown theory can be used to compute the true limit (e.g. 80%) for individual track sections and thus help to optimise track design.

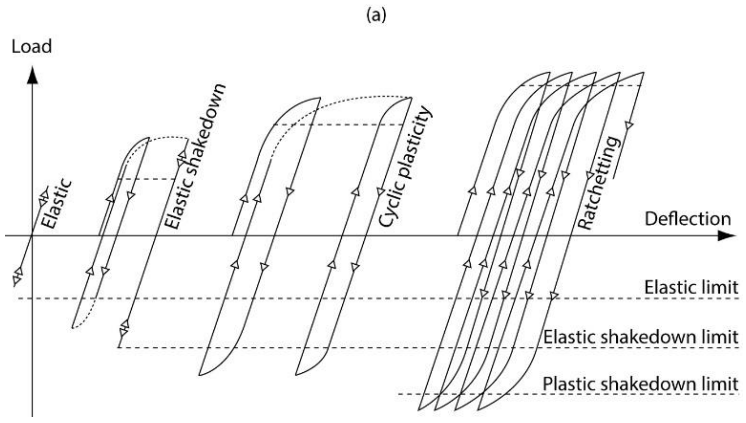

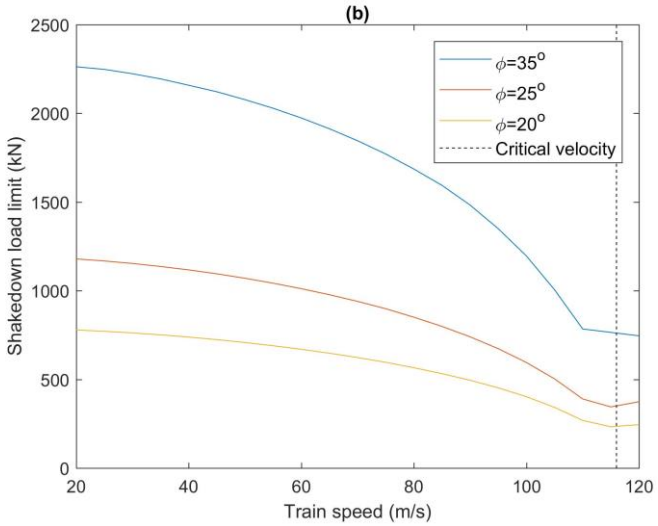

Figure 16. (a) elastic-perfectly plastic behaviour during cyclic loading (modified from [45]*), (b) speed versus shakedown limit*

3.11. Soil improvement

Two challenging scenarios may be detected during a critical velocity scoping study:

1. A low stiffness soil configuration which will likely require remediation (e.g. train speed > 70% of critical velocity, as defined during shakedown limit design)
2. A semi-low stiffness soil configuration for which the need for remediation is unclear (e.g. train speed between 50-70% of critical velocity, as defined during shakedown limit design)

3.11.1. Soil replacement

Assuming the preferred remediation method is soil replacement or improvement, it is necessary to determine the optimum depth and magnitude of stiffness improvement required, with respect to cost. This is challenging because the localised improvement of soil layers results in large stiffness contrasts, and increases the likelihood of the presence of sandwiched low stiffness layers which can cause multiple DAF peaks.

To illustrate this, Figure 17a shows the effect of soil replacement/remediation on maximum slab track deflections. The original soil is a homogenous half-space with 45MPa stiffness. The soil is then locally stiffened, considering 5 discrete depths (1, 2, 3, 4, 5m) and 3 magnitudes of stiffness improvement (100, 200, 300MPa). It is clear that the relationship between track deflection and improvement depth, as well as between track deflection and stiffness magnitude, are both non-linear relationships. Interestingly, deploying 1m of 300MPa improvement results in a minimal change in track deflection, while 1m of 100MPa and 200MPa improvement result in a magnification of rail displacement. This is because the train speed is marginally greater than the original soil critical velocity, and increasing the stiffness shifts the dynamic amplification peak closer to the train speed [41].

Considering the relationship between track deflection and the stiffness magnitude of replacement soil, except for the 1m depth case discussed above, the stiffer soil results in lower deflections. The relationship is complex though because different combinations of

stiffness and depth yield different levels of deflection. For example, 2m of 300MPa improvement gives a similar reduction in displacement as 5m of 100MPa improvement. Therefore, it is clear than when performing soil remediation, to minimise cost and maximise performance, it is important that both variables are considered.

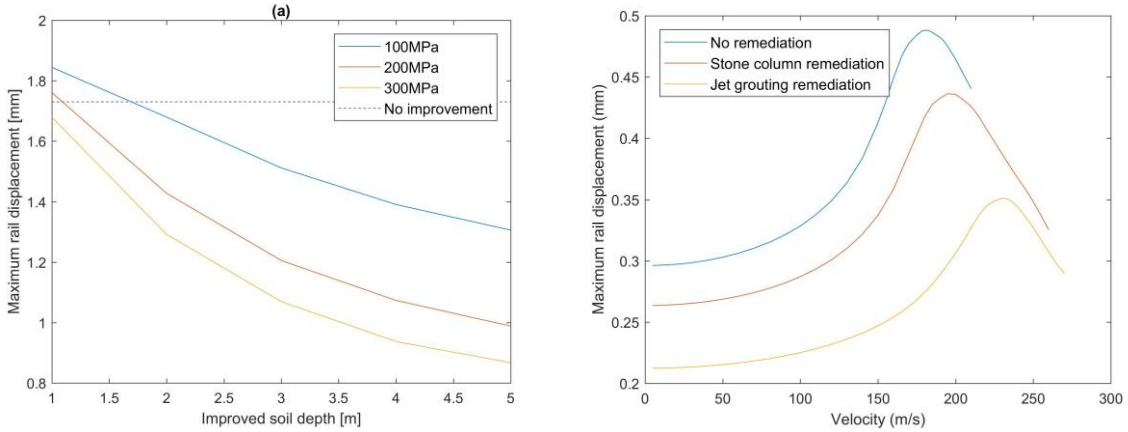

Figure 17. Soil improvement: (a) soil replacement optimisation (dashed line indicates 0m of improvement), (b) stone columns and jet grouting DAF

3.11.2 Discrete soil stiffening

Instead of using soil replacement to improve the dynamic characteristics of railway subgrade, stone columns or jet grouting can also be used. Figure 18 shows the improvement geometries of a 2 layer soil with stiffness's of 102 MPa and 468 MPa for the upper and lower layers respectively. The top soil layer is 4 m thick and the bottom layer is infinitely deep. The stone column solution consists of 9x0.8m diameter columns at 1.6 m spacing, with a stiffness of 160 MPa. Alternatively, the jet grouting solution consists of 5x0.7m diameter columns at 3.48 m spacing, with a stiffness of 1 GPa. Figure 17b shows the dynamic amplification curves for both solutions, compared against the non-remediated case. Note that they have been normalised with respect to the static displacement of the non-remediated case. Regarding critical velocity, the stone columns provide a 7% benefit, while the jet grouting provides a 22% benefit compared to the benchmark case. Similarly, regarding dynamic amplification, the stone columns provide a 12% benefit, while the jet grouting provides a 39% benefit. In a similar manner to the soil replacement considered previously, the stiffness, dimensions and quantity of stone columns or jet grouting have a significant effect on remediation cost/performance.

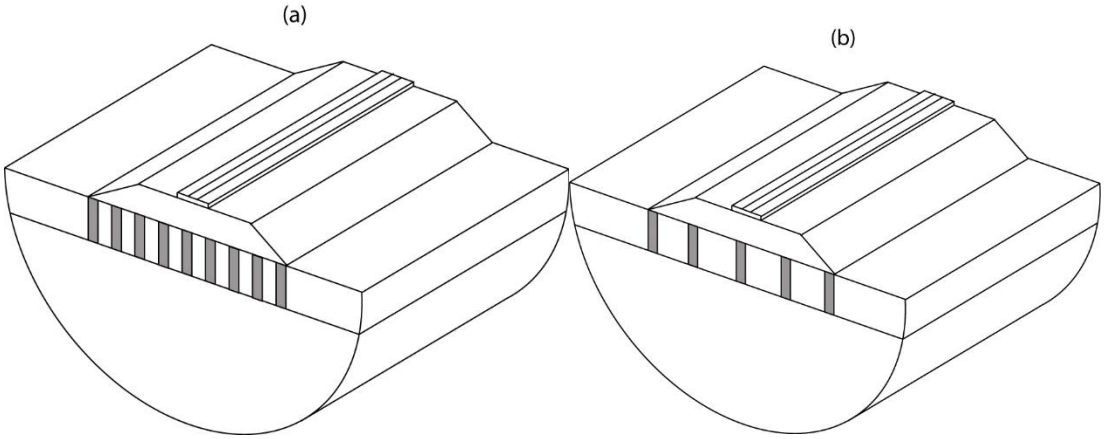

Figure 18. Discrete soil improvement: (a) Stone columns, (b) Jet grouting

4. Conclusion

This paper presents an analysis of a range of railway track dynamics problems. Firstly, the relatively straightforward issue of soil layering is presented, followed by problems of increasing technical difficulty, culminating in non-linear coupled track-soil analysis and soil remediation. Four linked models are used for the analysis: 1) an analytical model, 2) a combined analytical-numerical model, 3) a 2.5D finite element model, 4) a 3D finite element model.

It is found that changes to the dispersion relations for layered soils can cause a significant change in the critical velocity. Also, changes to the track structure can be used to increase the critical velocity, but only if the upper soil layer is not too deep. It is also found that bedrock depth plays an important role because small changes can have a significant effect on the critical velocity. It is found that low stiffness layers (either naturally occurring or engineered due to soil replacement) can significantly increase the complexity of soil wave dispersion and thus the critical velocity. The effect of vehicle wheel spacing is addressed and it is found that this is particularly important as train speeds approach (or exceed) the critical velocity. Finally, the effect of soil non-linearity and remediation solutions are investigated. It is shown that remediation is complex but can be designed with the support of elastodynamic models and shakedown theory. This allows for the design of track-ground structures with low dynamic amplification and minimal long-term permanent settlement.

Acknowledgements

The authors are grateful to the Leverhulme Trust (PLP-2016-270), the University of Leeds (including the Cheney fellowship scheme) the University of Porto and Heriot Watt University.

References

1 Alves Costa P, Colaço A, Calçada R, Cardoso AS. Critical speed of railway tracks. Detailed and simplified approaches. *Transp Geotech* Published Online First: September 2014. doi:10.1016/j.trgeo.2014.09.003

2 Woldringh RF, New BM. Embankment design for high speed trains on soft soils. In:

Proceedings of the 12th European Conference on Soil Mechanics and Geotechnical Engineering.Amsterdam, Netherlands: ; 1999. pp. 1703–1712.

3 Connolly DP, Alves Costa P, Kouroussis G, Galvin P, Woodward PK, Laghrouche O. Large Scale International Testing Of Railway Ground Vibrations Across Europe. *Soil Dyn Earthq Eng* 2015; **71**:1–12.

4 Wang P, Wei K, Wang L, Xiao J. Experimental study of the frequency-domain characteristics of ground vibrations caused by a high-speed train running on non-ballasted track. *Proc Inst Mech Eng Part F J Rail Rapid Transit* Published Online First: 2015. doi:10.1177/0954409715577849

5 Connolly DP, Kouroussis G, Woodward PK, Verlinden O, Alves Costa P, Forde MC. Field testing and analysis of high speed rail vibrations. *Soil Dyn Earthq Eng* 2014; **67**:102–118.

6 Krylov V, Dawson A, Heelis M, Collop A. Rail movement and ground waves caused by high-speed trains approaching track-soil critical velocities. *Proc Inst Mech Eng Part F J Rail Rapid Transit* 2000; **214**:107–116.

7 Noren-Cosgriff K, Berggren E, Kaynia AM, Dam N, Mortensen N. A new method for estimation of critical speed for railway tracks on soft ground. *Int J Rail Transp* 2018; :1–15.

8 Yu Z, Connolly DP, Woodward PK, Laghrouche O. True triaxial testing of geogrid for high speed railways. *Transp Geotech* 2019; **20**:2214–3912.

9 Galvín P, Mendoza DL, Connolly DP, Degrande G, Lombaert G, Romero A. Scoping assessment of free-field vibrations due to railway traffic. *Soil Dyn Earthq Eng* 2018; **114**:598–614.

10 Kouroussis G, Vogiatzis K, Connolly DP, Kouroussis G. Assessment of railway ground vibration in urban area using in-situ transfer mobilities and simulated vehicle-track interaction. *Int J Rail Transp* 2018; **6**:113–130.

11 López-Mendoza D, Connolly DP, Romero A, Kouroussis G, Galvín P. A transfer function method to predict building vibration and its application to railway defects. *Constr Build Mater* 2020; **232**. doi:10.1016/j.conbuildmat.2019.117217

12 Krylov V. *Ground Vibrations from High-Speed Railways: Prediction and mitigation*. ICE Publishing; 2019.

13 Thompson DJ, Kouroussis G, Ntotsios E, Thompson DJ, Kouroussis G. Modelling , simulation and evaluation of ground vibration caused by rail vehicles caused by rail vehicles. *Veh Syst Dyn* 2019; **57**:936–983.

14 Takemiya H. Simulation of track–ground vibrations due to a high-speed train: the case of X-2000 at Ledsgard. *J Sound Vib* 2003; **261**:503–526.

15 Kaynia AM, Madshus C, Zackrisson P. Ground vibration from high speed trains - prediction and countermeasure. *J Geotech Geoenvironmental Eng* 2000; **126**:531–537.

16 Madshus C, Kaynia AM. High-Speed Railway Lines on Soft Ground: Dynamic Behaviour At Critical Train Speed. *J Sound Vib* 2000; **231**:689–701.

17 Holm G, Andreasson B, Bengtsson P, Bodare A, Eriksson H. Mitigation of Track and Ground Vibrations by High Speed Trains at Ledsgard, Sweden. Report 10. ; 2002.

18 Dyk BJ Van, Edwards JR, Dersch MS, Jr CJR, Barkan CPL. Evaluation of dynamic and impact wheel load factors and their application in design processes. *Proc Inst*

Mech Eng Part F J Rail Rapid Transit 2017; **231**:33–43.

19 Kenney J. Steady-state vibrations of beam on elastic foundation for moving load. *J Appl Mech* 1954; **76**:359–364.

20 Fryba L. *Vibration of Solids and Structures Under Moving Loads*. Groningen, The Netherlands: Noordhoff International Publishing; 1972.

21 Lamb H. On the propagation of tremors over the surface of an elastic solid. *Philos Trans R Soc London Ser A, Contain Pap a Math or Phys Character* 1904; **203**:1–42.

22 Mezher SB, Connolly DP, Woodward PK, Laghrouche O, Pombo J, Costa PA. Railway critical velocity - Analytical prediction and analysis. *Transp Geotech* 2016; **6**:84–96.

23 Dieterman H, Metrikine A. The Equivalent stiffness of a half-space interacting with a beam. Critical velocities of a moving load along the beam. *Eur J Mech - A/Solids* 1996; **15**:67–90.

24 Barros F, Luco JE. Stresses and displacements in a layered half-space for a moving line load. *Appl Math Comput* 1995; **67**:103–134.

25 Sheng X, Jones CJC, Thompson DJ. A comparison of a theoretical model for quasi-statically and dynamically induced environmental vibration from trains with measurements. *J Sound Vib* 2003; **267**:621–635.

26 Lombaert G, Degrande G, Kogut J, Francois S. The experimental validation of a numerical model for the prediction of railway induced vibrations. *J Sound Vib* 2006; **297**:512–535.

27 Hung HH, Chen GH, Yang YB. Effect of railway roughness on soil vibrations due to moving trains by 2.5D finite/infinite element approach. *Eng Struct* 2013; **57**:254–266.

28 Alves Costa P, Calcada R, Cardoso AS, Bodare A. Influence of soil non-linearity on the dynamic response of high-speed railway tracks. *Soil Dyn Earthq Eng* 2010; **30**:221–235.

29 Barbosa J, Park J, Kausel E. Perfectly matched layers in the thin layer method. *Comput Methods Appl Mech Eng* 2012; **217**–**220**:262–274.

30 Arlaud E, Costa D'Aguiar S, Balmes E. Receptance of railway tracks at low frequency: Numerical and experimental approaches. *Transp Geotech* 2016; **9**:1–16.

31 Chebli H, Othman R, Clouteau D, Arnst M, Degrande G. 3D periodic BE – FE model for various transportation structures interacting with soil. *Comput Geotech* 2008; **35**:22–32.

32 de Abreu Corrêa L, Quezada JC, Cottereau R, d'Aguiar SC, Voivret C. Randomly-fluctuating heterogeneous continuum model of a ballasted railway track. *Comput Mech* 2017; **60**:845–861.

33 Galvin P, Romero A, Domínguez J. Fully three-dimensional analysis of high-speed train–track–soil-structure dynamic interaction. *J Sound Vib* 2010; **329**:5147–5163.

34 Hall L. Simulations and analyses of train-induced ground vibrations in finite element models. *Soil Dyn Earthq Eng* 2003; **23**:403–413.

35 Olivier B, Connolly DP, Alves Costa P, Kouroussis G. The effect of embankment on high speed rail ground vibrations. *Int J Rail Transp* 2016; **4**:229–246.

36 Connolly D, Giannopoulos A, Fan W, Woodward PK, Forde MC. Optimising low acoustic impedance back-fill material wave barrier dimensions to shield structures

from ground borne high speed rail vibrations. *Constr Build Mater* 2013; **44**:557–564.

37 Varandas JN, Hölscher P, Silva M. Dynamic behaviour of railway tracks on transitions zones. *Comput Struct* 2011; **89**:1468–1479.

38 Shih JY, Thompson DJ, Zervos A. The influence of soil nonlinear properties on the track/ground vibration induced by trains running on soft ground. *Transp Geotech* 2017; **11**:1–16.

39 Woodward PK, Laghrouche O, Mezher SB, Connolly DP. Application of coupled train-track modelling of critical speeds for high-speed trains using three-dimensional non-linear finite elements. *Int J Railw Technol* 2015; **4**:1–35.

40 Colaço A, Costa PA, Connolly DP. The influence of train properties on railway ground vibrations. *Struct Infrastruct Eng* 2015; :1–18.

41 Dong K, Connolly DP, Laghrouche O, Woodward PK, Costa PA. The stiffening of soft soils on railway lines. *Transp Geotech* 2018; **17**:178–191.

42 Connolly D, Giannopoulos A, Forde MC. Numerical modelling of ground borne vibrations from high speed rail lines on embankments. *Soil Dyn Earthq Eng* 2013; **46**:13–19.

43 Kouroussis G, Verlinden O. Prediction of railway ground vibrations: Accuracy of a coupled lumped mass model for representing the track/soil interaction. *Soil Dyn Earthq Eng* 2015; **69**:220–226.

44 Brown SF. Soil mechanics in pavement engineering. *Geotechnique* 1996; **46**:383–426.

45 Collins IF, Boulbibane M. Geomechanical analysis of unbound pavements based on shakedown theory. *J Geotech Geoenvironmental Eng* 2000; **126**:50–59.

46 Connolly DP, Alves Costa P. Geodynamics of very high speed transport systems. *Soil Dyn Earthq Eng* 2020; **130**:105982.

47 Kouroussis G, Connolly DP, Verlinden O. Railway induced ground vibrations - a review of vehicle effects. *Int J Rail Transp* 2014; **2**:69–110.

48 Dong K, Connolly DP, Laghrouche O, Woodward PK, Alves Costa P. Non-linear Soil Behaviour on High Speed Rail Lines. *Comput Geotech* 2019; **112**:302–318.

49 Yu Z, Connolly DP, Woodward PK, Laghrouche O. Settlement behaviour of hybrid asphalt-ballast railway tracks. *Constr Build Mater* 2019; **208**:808–817.

50 Boulbibane M, Collins IF, Weichert D, Raad L. Shakedown analysis of anisotropic asphalt concrete pavements with clay subgrade. *Can Geotech J* 2000; **37**:882–889.

51 Brown SF, Yu HS, Juspi S, Wang J. Validation experiments for lower-bound shakedown theory applied to layered pavement systems. *Géotechnique* 2012; **62**:923–932.

52 Yu HS, Wang J. Three-dimensional shakedown solutions for cohesive-frictional materials under moving surface loads. *Int J Solids Struct* 2012; **49**:3797–3807.

53 Alves Costa P, Lopes P, Silva Cardoso A. Soil shakedown analysis of slab railway tracks: Numerical approach and parametric study. *Transp Geotech* 2018; **16**:85–96.